INTL JOURNAL OF ELECTRONICS AND TELECOMMUNICATIONS, 2024, VOL. 70, NO. 3, PP. 683-690
Manuscript received February 26, 2024; revised July, 2024. doi: 10.24425/ijet.2024.149597

Resonant Frequencies of TE_{0mn} modes in multilayered resonators containing uniaxial anisotropic dielectrics with complex shapes

Krzysztof Derzakowski

***Abstract*—The method of evaluating the resonant frequencies of multilayered resonator containing uniaxial anisotropic dielectrics is presented. The detailed solution of Maxwell's equations for such a structure by means of the radial modes matching method for TE_{0mn} modes is given. The results of calculations using developed and launched computer program are given. Results of calculations are compared with those obtained by other method using CST simulator. These results are in close agreement, which proves the correctness of the method. The developed solution, and the software program can be used to measure the tensor permittivity of dielectrics.**

***Keywords*—dielectric resonator; Maxwell's equations; radial modes matching method; uniaxial anisotropic permittivity**

I. Introduction

THE development of materials technology makes that newly created materials have previously unattainable electrical and magnetic properties. Materials produced and used in electronics have a wide range of relative permittivity and permeability. These parameters may vary depending on the frequency as well as a function of the direction (anisotropic dielectric, ferrites). The use of such materials in electronics enforces the need for accurate knowledge of their electrical and magnetic parameters. It is therefore necessary to develop newer and better methods to measure these materials.

At microwave frequencies, resonant methods are most often used, in particular dielectric resonator method [1]. The advantage of this method is very good accuracy to determine material parameters, as well as measurements are easy. The resonant frequency and the Q-factor of structure, which includes sample test material are measured at once [2]. The material parameters are determined from the equations describing the resonance conditions of the test structure. The most commonly used is TE_{011} mode [1]. In measurements, not very complicated structures are used [1],[3].

In microwave devices (filters, antennas) using dielectric resonators containing various materials, different complicate shapes of structures can be used [4]-[16]. The following examples of the shapes of dielectric resonators limited to axisymmetric ones can be found:
- cylindrical or disc [4],[5],
- disc with curved edge [6],
- wedge disc [6],[7],
- ring [8],
- toroid [6],[7],
- split cylinders (SPDR) and rings [9],[10],
- triple layer cylindrical and ring resonators [11]-[13],
- spherical and hemispherical [6],[7],[14]-[16],
- conical [14],

It follows from the above that it is necessary to be able to determine the resonant frequency of TE_{0mn} modes for complex structures containing materials with different electrical properties. There are many ways to derive these frequencies, however, most accurate appear to be modes matching methods, either radial or axial

There are numerous of studies to enable the calculation of the resonant frequency of such structure, but most commonly they involve simple structure composed of a small number of layers of a material [3],[18]-[21]. The most advanced solution relates to a multilayered dielectric resonator which can contain up to 10 regions and 10 layers in each of them, but dielectrics included in the system are described by scalar relative permittivity [20]. In [22] you can find a solution for a structure consisting of 20 regions and 20 layers of dielectrics in each of them determined by tensor electric permittivity for all modes. However, using the solution from [22] requires some experience to distinguish between the TE and TM modes. Therefore, this article limits the solution to TE modes, but increases the number of regions and layers to 50.

You can use any electromagnetic simulator, e.g. CST [23], HFFS [24], QuickWave [25], to calculate the resonant frequency of a complex structure. However, each of these simulators use approximations of partial differential equations, so the accuracy of the calculations is limited. In the 3D simulators the structure is meshed and accuracy of the computations depends on the mesh size. Thus the accuracy depends on the quantization of space. It can also depends on the quantization of time (in FDTD), dispersion, round-off errors etc. The computation time in some simulators may be much longer than in the presented solution. The price of commercial electromagnetic simulators is also an important factor but it must be added that the 3D electromagnetic simulators can be used to any type of structures, which is their main advantage.

In this paper, a solution employing the radial modes matching method for the multilayered resonator containing dielectrics

Krzysztof Derzakowski is with Institute of Radioelectronics and Multimedia Technology, Warsaw University of Technology, Poland (e-mail: Krzysztof.Derzakowski@pw.edu.pl).

determined by tensor permittivity for TE_{0mn} modes is presented. The solution of the Maxwell equations for the multilayered resonator, which may contain up to 50 regions and 50 layers of each of them, which is more than exhaustive demand is presented.

The simplified general structure of the multilayered dielectric resonator is shown in Fig. 1.

It consists of three regions I, II and III with axial symmetry. The amount of these regions can be equal to a maximum of 50 in the developed program. The first region thus has a cylindrical shape, the next ones are rings. In each region there is a number of layers of material having different relative tensor permittivity. The structure is enclosed by a metal cylinder whose radius R_3 may be infinite. The structure does not affect constant or slowly varying external magnetic field.

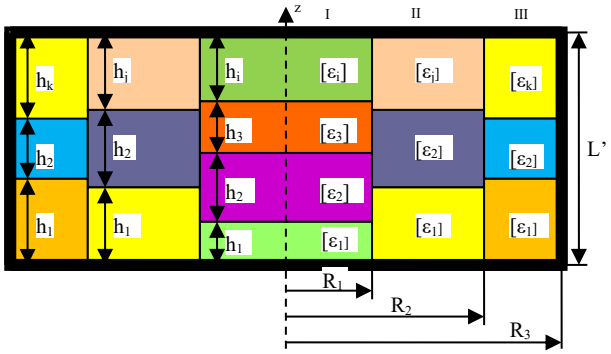

Fig. 1. The multilayered dielectric resonator

II. THE SOLUTION OF BOUNDARY VALUE PROBLEM FOR THE RESONATOR WITH ANISOTROPIC MEDIA

Stated problem boils down to solve Maxwell's equations for such a structure. Due to the rotational symmetry of the analyzed structure the Maxwell equations will be solved in a cylindrical coordinate system.

Maxwell's equations in each layer of each region can be written as (given the absence of charges and currents sources):

$$\begin{cases} \nabla \times \vec{E} = j\omega \vec{B} & (1) \\ \nabla \times \vec{H} = j\omega \vec{D} & (2) \\ \nabla \cdot \vec{D} = 0 & (3) \\ \nabla \cdot \vec{B} = 0 & (4) \end{cases}$$

Taking into account the linearity and dielectric anisotropy of the media belonging to the resonator the following are obtained:

$$\begin{cases} \nabla \times \vec{E} = j\omega\mu \vec{H} & (5) \\ \nabla \times \vec{H} = j\omega [\varepsilon] \vec{E} & (6) \\ \nabla \cdot ([\varepsilon])\, \vec{E} = 0 & (7) \\ \nabla \cdot \mu \vec{H} = 0 & (8) \end{cases}$$

where: $[\varepsilon] = \begin{bmatrix} \varepsilon_t & 0 & 0 \\ 0 & \varepsilon_t & 0 \\ 0 & 0 & \varepsilon_z \end{bmatrix}$ is a uniaxial anisotropic permittivity.

For TE_{0mn} modes, the electric field $\vec{E}$ and magnetic field $\vec{H}$ vectors take the following form: $\vec{E} = [0,0,E_\varphi]$, $\vec{H} = [H_r, H_z, 0]$.

It was also assumed that the non-zero components of these vectors are independent of the angle φ.

We transform (5-8) using vector calculus and finally obtain (9):

$$\nabla(\nabla \cdot \vec{E}) - \nabla^2 \vec{E} = \omega^2 \mu_0 [\varepsilon] \vec{E} \qquad (9)$$

The value of the electric field divergence is determined from (7). And we obtain (10)

$$\nabla \cdot ([\varepsilon])\, \vec{E} = \varepsilon_t \nabla \cdot \vec{E} \; - \varepsilon_t \left(1 - \frac{\varepsilon_z}{\varepsilon_t}\right) \frac{\partial E_z}{\partial z} \qquad (10)$$

The left side of the above equation must be equal to zero (from (7)), so we can write (11):

$$\nabla \cdot \vec{E} = \left(1 - \frac{\varepsilon_z}{\varepsilon_t}\right) \frac{\partial E_z}{\partial z} \qquad (11)$$

Substituting into (9) we get:

$$\left(1 - \frac{\varepsilon_z}{\varepsilon_t}\right) \nabla \frac{\partial E_z}{\partial z} - \nabla^2 \vec{E} = \omega^2 \mu_0 [\varepsilon] \vec{E} \qquad (12)$$

Writing (12) in a cylindrical coordinate system and using the properties of the Laplacian and taking into account the form of vectors $\vec{E}$ and $\vec{H}$, after simple transformations, we obtain (13):

$$\frac{\partial^2 E_\varphi}{\partial z^2} + \frac{\partial}{\partial r}\left[\frac{1}{r}\frac{\partial}{\partial r}\left(r E_\varphi\right)\right] - \frac{E_\varphi}{r^2} + k_0^2 \varepsilon_t E_\varphi = 0 \qquad (13)$$

where: $k_0 = \omega_0 \sqrt{\varepsilon_0 \mu_0} = \frac{2\pi}{\lambda_0}$.

The equation (13) is solved separately in each layer of each of the region by using the method of separation of variables, and then the solutions are "stitched" on the borders of regions (r = R_1, R_2, R_3…), ensuring continuity of tangential components.

Assuming that in (13) $E_\varphi(r,z) = U(r) * \Phi(z)$, a system of two equations of a single variable is obtained:

$$\begin{cases} \dfrac{d^2\Phi(z)}{dz^2} + [k_0^2 \varepsilon_t - \lambda_m]\Phi(z) = 0 & (14) \\ r^2 \dfrac{d^2 \mathrm{U}(r)}{dr^2} + r \dfrac{\mathrm{dU}(r)}{dr} + (\lambda_m r^2 - 1)\mathrm{U}(r) = 0 & (15) \end{cases}$$

Equation (15) is the first-order Bessel equation for $\lambda_m > 0$, and the first-order modified Bessel equation for $\lambda_m < 0$. Its solutions for $\lambda_m > 0$ are Bessel functions of the first kind - $J_1\left(\sqrt{\lambda_m} r\right)$ and Neuman functions (Bessel functions of the second kind) - $N_1\left(\sqrt{\lambda_m} r\right)$. And for $\lambda_m < 0$. solutions of (15) are modified Bessel functions of the first kind - $I_1\left(\sqrt{\lambda_m} r\right)$ and the second kind - $K_1\left(\sqrt{\lambda_m} r\right)$. It should be noticed that for the I-st region taking into account the Neuman function is not justified physically.

In each layer of a given region, the tensor permittivity is constant and the solutions of (14) are the functions $\Phi_m(z)$ which are a linear combination of trigonometric functions of the type $\sin\left(v_{m_i} z\right)$ and $\cos\left(v_{m_i} z\right)$. Where: $v_{m_i}^2 = k_0^2 - \lambda_m$:

If $v_{m_i}^2 < 0$, the trigonometric functions should be replaced with appropriate hyperbolic functions, i.e. $\sinh\left(v_{m_i} z\right)$ and $\cosh\left(v_{m_i} z\right)$.

Since the $\Phi_m(z)$ functions must be defined over the entire height of a given region, appropriate continuity conditions must be ensured on the electrical walls and on the separation planes of individual layers, i.e. $\Phi^-(l_i) = \Phi^+(l_i)$ and $\Phi(0) = \Phi(L')$. where: $\Phi^-(l_i), \Phi^+(l_i)$ - are values of a function Φ on the left and right side of the boundary, and $\Phi(0), \Phi(L')$. – are values of Φ on the lower and upper metal plate.

The E_φ and H_z field components in each region are a linear combination of waveguide modes, so the relationships for the electromagnetic field components can be written (assuming that the radius of the third area extends to infinity):

$$E_\varphi^I(r,z) = \sum_{i=0}^{\infty} \frac{a_m}{\sqrt{\lambda_m^I}} J_1\left(\sqrt{\lambda_i^I} r\right) \Phi_m^I(z) \tag{16}$$

$$E_\varphi^{II}(r,z) = \sum_{i=0}^{\infty} \left[\frac{b_m}{\sqrt{\lambda_m^{II}}} J_1\left(\sqrt{\lambda_i^{II}} r\right) + \frac{c_m}{\sqrt{\lambda_m^{II}}} N_1\left(\sqrt{\lambda_i^{II}} r\right) \right] \Phi_m^{II}(z) \tag{17}$$

$$E_\varphi^{III}(r,z) = \sum_{i=0}^{\infty} \frac{d_m}{\sqrt{\lambda_m^{III}}} K_1\left(\sqrt{\lambda_i^{III}} r\right) \Phi_m^{III}(z) \tag{18}$$

$$H_z^I(r,z) = \frac{j}{\omega\mu_0} \sum_{i=0}^{\infty} a_m J_0\left(\sqrt{\lambda_i^I} r\right) \Phi_m^I(z) \tag{19}$$

$$H_z^{II}(r,z) = \frac{j}{\omega\mu_0} \sum_{i=0}^{\infty} \left[b_m J_0\left(\sqrt{\lambda_i^{II}} r\right) + c_m N_0\left(\sqrt{\lambda_i^{II}} r\right) \right] \Phi_m^{II}(z) \tag{20}$$

$$H_z^{III}(r,z) = \frac{j}{\omega\mu_0} \sum_{i=0}^{\infty} \frac{d_m}{\sqrt{\lambda_m^{III}}} K_0\left(\sqrt{\lambda_i^{III}} r\right) \Phi_m^{III}(z) \tag{21}$$

where: a_m, b_m, c_m and d_m are complex constants,

Due to the negligibly small values of the higher components of the series, the summation can be limited to a finite number of elements N. The coefficients a_m, b_m, c_m and d_m should be selected to ensure the continuity of the electromagnetic field at the boundaries of the regions, i.e. to:

$$H_z^I(R_1,z) - H_z^{II}(R_1,z) = 0 \tag{22}$$

$$E_\varphi^I(R_1,z) - E_\varphi^{II}(R_1,z) = 0 \tag{23}$$

$$H_z^{II}(R_2,z) - H_z^{III}(R_2,z) = 0 \tag{24}$$

$$E_\varphi^{II}(R_2,z) - E_\varphi^{III}(R_2,z) = 0 \tag{25}$$

In the case of a finite number of terms fulfilling the conditions of equality is impossible for all z. Therefore, these coefficients are determined from the condition that the mean square error (functional) component of the difference on either side of the boundary reached the minimum value. The corresponding functionals have the form (here written for the three regions):

$$F_1 = \int_S |H_z^I(R_1,z) - H_z^{II}(R_1,z)|^2 \, ds \tag{26}$$

$$F_2 = \int_S \left|E_\varphi^I(R_1,z) - E_\varphi^{II}(R_1,z)\right|^2 \, ds \tag{27}$$

$$F_3 = \int_S |H_z^{II}(R_2,z) - H_z^{III}(R_2,z)|^2 \, ds \tag{28}$$

$$F_4 = \int_S \left|E_\varphi^{II}(R_2,z) - E_\varphi^{III}(R_2,z)\right|^2 \, ds \tag{29}$$

Functionals achieve these minimum values if and only if their derivatives with respect to unknown coefficients are equal to zero (Rayleigh-Ritz method). After differentiating F_1 with respect to a_m, F_2 with respect to b_m, F_3 with respect to c_m and F_4 with respect to d_m, a system of 4N linear equations is obtained, allowing the determination of the unknown constants a_m, b_m, c_m and d_m (30).

$$\widetilde{W} \begin{bmatrix} a_1 \\ a_2 \\ \cdots \\ d_m \end{bmatrix} = 0 \tag{30}$$

This system has a non-zero solution if and only if its determinant is equal to zero

$$det\widetilde{W} = 0 \tag{31}$$

The matrix $\widetilde{W}$ with dimensions 4Nx4N, for three regions, has the form (32), and its elements are presented in Table I.

$$\widetilde{W} = \begin{bmatrix} U_1 & U_2 & U_3 & U_4 \\ U_5 & U_6 & U_7 & U_8 \end{bmatrix} \tag{32}$$

where: U_4 and U_5 are matrices with zero elements, and the remaining matrices have the form of $U_i = [v^{i1} \quad v^{i2}]^T$.

TABLE I
ELEMENTS OF W MATRIX FOR THREE REGIONS

i	$v_{qk}^{i1}(q,k = 1,2,\dots N)$	$v_{qk}^{i2}(q,k = 1,2,\dots N)$
1	$J_0\left(h_i^I R_1\right)\langle\Phi_k^I(z)\Phi_q^{I*}(z)\rangle$	$\frac{J_1\left(h_i^I R_1\right)}{h_i^I}\langle\Phi_k^I(z)\Phi_q^{II*}(z)\rangle$
2	$J_0\left(h_i^{II} R_1\right)\langle\Phi_k^{II}(z)\Phi_q^{I*}(z)\rangle$	$\frac{J_1\left(h_i^{II} R_1\right)}{h_i^{II}}\langle\Phi_k^{II}(z)\Phi_q^{II*}(z)\rangle$
3	$N_0\left(h_i^{II} R_1\right)\langle\Phi_k^{II}(z)\Phi_q^{I*}(z)\rangle$	$\frac{N_1\left(h_i^{II} R_1\right)}{h_i^{II}}\langle\Phi_k^{II}(z)\Phi_q^{II*}(z)\rangle$
6	$J_0\left(h_i^{II} R_2\right)\langle\Phi_k^{II}(z)\Phi_q^{II*}(z)\rangle$	$\frac{J_1\left(h_i^{II} R_2\right)}{h_i^{II}}\langle\Phi_k^{II}(z)\Phi_q^{III*}(z)\rangle$
7	$N_0\left(h_i^{II} R_2\right)\langle\Phi_k^{II}(z)\Phi_q^{II*}(z)\rangle$	$\frac{N_1\left(h_i^{II} R_2\right)}{h_i^{II}}\langle\Phi_k^{II}(z)\Phi_q^{III*}(z)\rangle$
8	$K_0\left(h_i^{III} R_2\right)\langle\Phi_k^{III}(z)\Phi_q^{II*}(z)\rangle$	$\frac{-K_1\left(h_i^{III} R_2\right)}{h_i^{III}}\langle\Phi_k^{III}(z)\Phi_q^{III*}(z)\rangle$

where: $\langle \Phi_k^{(\alpha)}(z)\Phi_q^{(\beta)}(z)\rangle = \int_0^{L'} \Phi_k^{(\alpha)}(z)\Phi_q^{(\beta)}(z)\,dz$, and $h_i^{(\alpha)} = \sqrt{\lambda_i^{(\alpha)}}$.

III. Results and Discussion

This section presents the results of the calculations of the resonant frequency of the TE_{0mn} modes of a resonator in the form of a cylinder and a cone. The simulations started with determining the resonant frequencies of various TE_{0mn} modes for a cylindrical resonator placed in a metal cavity with a height equal to the height of the resonator and a radius much larger than the radius of the cylinder. The geometric dimensions and electrical parameters of the resonator were identical to those in [21], i.e. height h_d = 8.998 mm, diameter r_d = 9.995 mm, relative longitudinal electrical permittivity ε_z = 9.389, transverse permittivity ε_t = 11.478. For such a structure, determining the resonant frequency is very simple and does not require advanced methods. The results of calculations are shown in Table II. This table also presents the calculation results for two other structures and the results presented in the literature. The results are almost identical.

Table II
The comparison of resonant frequencies of TE_{011} mode [GHz]

Sample	Publication [xy]	Measurement	This method
1	9.720 [21]	9.714	9.719
2	10.704 [21]	10.706	10.704
3	8.5405 [18]	-	8.5421

Sample no. 1: diameter D = 9.985 mm, height L = 9.998 mm, ε_t =9.389, ε_z =11.478, centrally placed within a metal cylinder having a diameter d = 15.5 mm, height h = 13 mm with stands of the same diameter as the sample located on both sides of the sample, the height l_l = 1.501 mm and a relative permittivity ε_l =1.031.

Sample no. 2: diameter D = 10.002 mm, height L = 5.002 mm, ε_t =9.399, ε_z =11.553, located centrally in the cylinder identical as for sample no.1 with stands of the same diameter as the sample located on both sides of the sample, the amount l_l = 3.999 mm and a relative permittivity ε_l =1.031.

Sample no. 3: diameter D = 37.7 mm, height L = 9.4 mm, ε_t =4.43, ε_z =4.59, centrally placed within a metal cylinder having a diameter d = 140 mm and height h = 9.4 mm

For the structure presented earlier, the resonant frequencies of the TE_{0mn} modes were calculated by changing the elements of the permittivity tensor. The results are presented in Figs 2 and 3. As can be seen from Fig.2, the resonant frequencies do not change as a function of the longitudinal component of permittivity ε_z. This result is correct because the electromagnetic field components for these modes do not depend on ε_z.

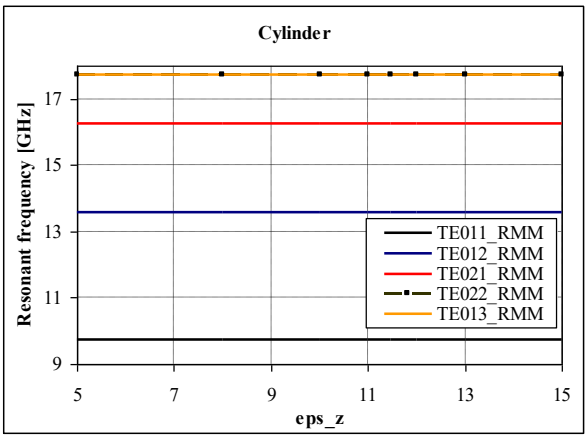

Fig. 2. Resonant frequency as a function of the permittivity ε_z for uniaxial anisotropic dielectric cylindrical resonator obtained by means of radial modes matching method (RMM)

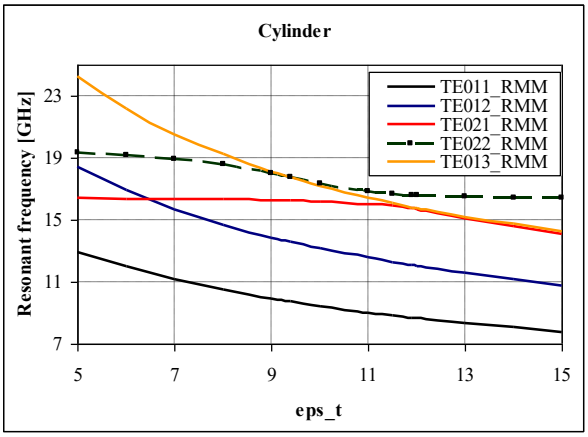

Fig. 3. Resonant frequency as a function of the permittivity ε_t for uniaxial anisotropic dielectric cylindrical resonator obtained by means of radial modes matching method (RMM)

For comparison, Figs 4 and 5 show the results obtained using the CST electromagnetic simulator. As you can see, the results are almost identical. Figs 6 and 7 show the relative difference in frequencies calculated by both programs - R_f. This difference was defined as (33):

$$R_f = \frac{f_{RMM} - f_{CST}}{f_{CST}} \cdot 100\ [\%] \tag{33}$$

where: R_f – the relative difference of frequencies, f_{RMM} – the resonant frequency obtained by means of the radial modes matching method, f_{CST} – the resonant frequency obtained by means of the CST electromagnetic simulator.

As seen in Fig. 6, R_f varies from 0 to 0.3 percent with the change of ε_z and from 0 to 0.7 percent as a function of ε_t for TE_{011} mode. For other modes, the R_f coefficient does not exceed 1 percent. This is a very good agreement between the obtained results, especially considering the relationship between the resonant frequency calculated by the CST simulator and the place of resonator excitation.

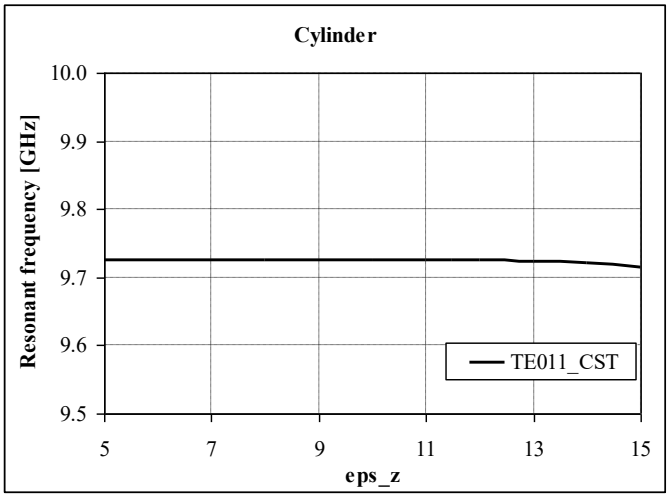

Fig. 4. Resonant frequency as a function of the permittivity ε_z for uniaxial anisotropic dielectric cylindrical resonator obtained by means of CST simulator

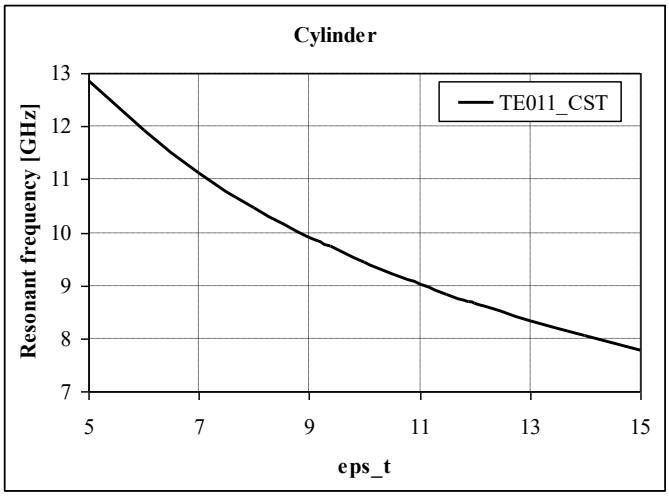

Fig. 5. Resonant frequency as a function of a permittivity ε_t for uniaxial anisotropic dielectric cylindrical resonator obtained by means of CST simulator

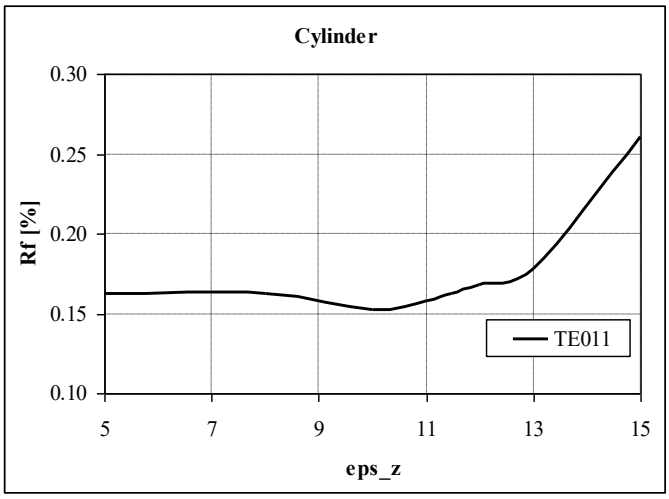

Fig. 6. The coefficient R_f as a function of the permittivity ε_z for uniaxial anisotropic dielectric cylindrical resonator

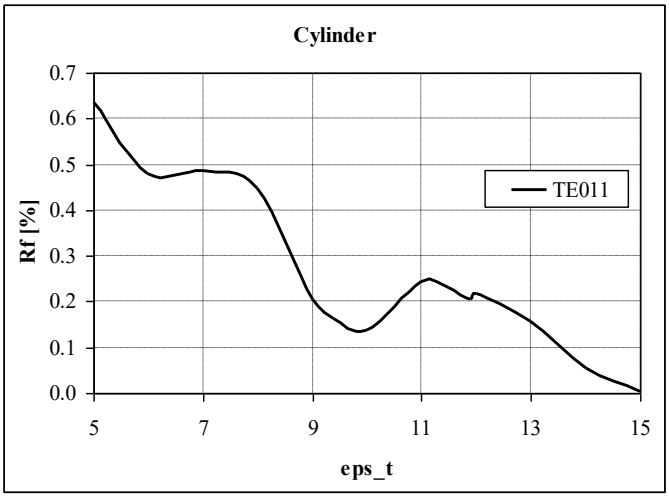

Fig. 7. The coefficient R_f as a function of the permittivity ε_t for uniaxial anisotropic dielectric cylindrical resonator

In the radial modes matching method, a complex structure can be obtained by dividing it into regions and layers that are cylinders and rings. This division for a cone shaped resonator is shown in Fig. 8.

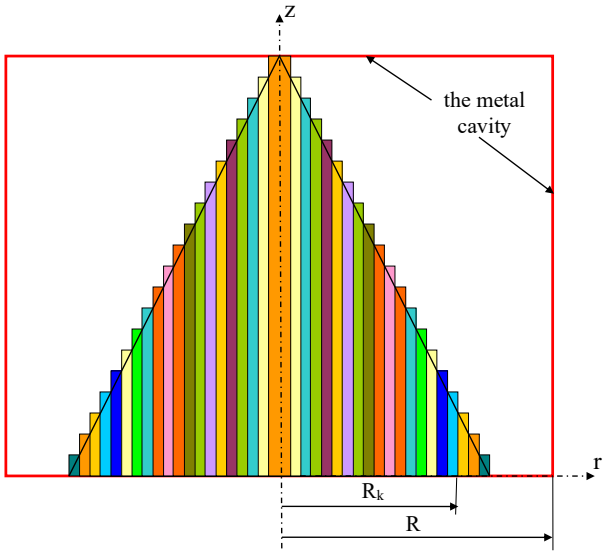

Fig. 8. The approximation of the conical resonator in the radial modes matching method

According to the rules of the radial modes matching method, the structure was divided into N + 1 regions, with N regions creating the space of the cone. The radii of the regions were determined assuming that the height of the cone will be divided into N parts (h_N) and that each region will have a height equal to the multiple of the value h_N. Hence, the dependence on the radius of a given region is obtained in the form (34):

$$R_i = R_c - (N - i - 1) \cdot h_N \cdot \frac{(R_c - R_1)}{L_c - h_N} \tag{34}$$

where: R_i – is a radius of *i* region, N – numbers of regions in a cone, R_c – the radius of base of a cone, R_1 – the radius of first region, L_c – the height of a cone, $h_N = L_c/N$.

An example of the values of the heights and radii of the regions of the approximated conical resonator divided into 30 regions is presented in Table III.

TABLE III
AN APPROXIMATION OF A CONE IN PRESENTED METHOD

i	Radius [mm]	Height [mm]
1	0.05	9.998000000
2	0.220431034	9.664733333
3	0.390862069	9.331466667
4	0.561293103	8.998200000
5	0.731724138	8.664933333
6	0.902155000	8.331666667
7	1.072586000	7.998400000
8	1.243017000	7.665133333
9	1.413448000	7.331866667
10	1.583879000	6.998600000
11	1.754310000	6.665333333
12	1.924741000	6.332066667
13	2.095172000	5.998800000
14	2.265603000	5.665533333
15	2.436034000	5.332266667
16	2.606466000	4.999000000
17	2.776897000	4.665733333
18	2.947328000	4.332466667
19	3.117759000	3.999200000
20	3.28819000	3.665933333
21	3.458621000	3.332666667
22	3.629052000	2.999400000
23	3.799483000	2.666133333
24	3.969914000	2.332866667
25	4.140345000	1.999600000
26	4.310776000	1.666333333
27	4.481207000	1.333066667
28	4.651638000	0.999800000
29	4.822069000	0.666533333
30	4.992500000	0.333266667

The accuracy of mapping the conical resonator by such division depends on the number of regions. Therefore, calculations were carried out for various numbers of regions in order to determine the number of ones enabling a sufficient approximation of the cone. The results of these calculations are presented in Figs 9 and 10.

R_k values defined as the relative difference in the resonant frequency for a specific value of the number of regions in relation to the maximum number of these regions – 50, are described by the formula (35):

$$R_k = \frac{f_i - f_{max}}{f_{max}} \cdot 100\ [\%] \tag{35}$$

where: R_k – the relative difference of frequencies, f_{max} – the resonant frequency obtained for maximum number of regions, f_i – the resonant frequency obtained for i region.

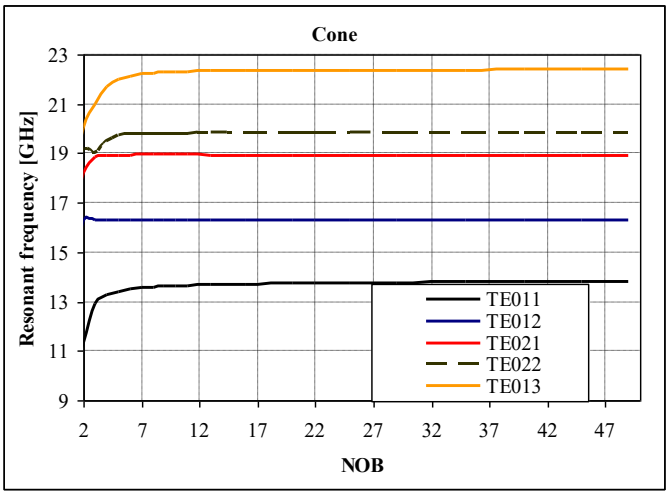

Fig. 9. Resonant frequencies as a function of number of regions in radial modes matching method (RMM)

As can be seen from Fig. 9, as the number of regions increases, the values of the calculated resonant frequencies stabilize towards the asymptotic value. This is clearly visible in Fig. 10, where for the number of regions above 30, changes in resonant frequencies do not exceed 0.1 percent for all TE_{0mn} modes.

Similarly to the cylinder, calculations were made for a conical resonator (N = 40) as a function of both permittivities for five TE_{0mn} modes. The results are presented in Figs 11 and 12.

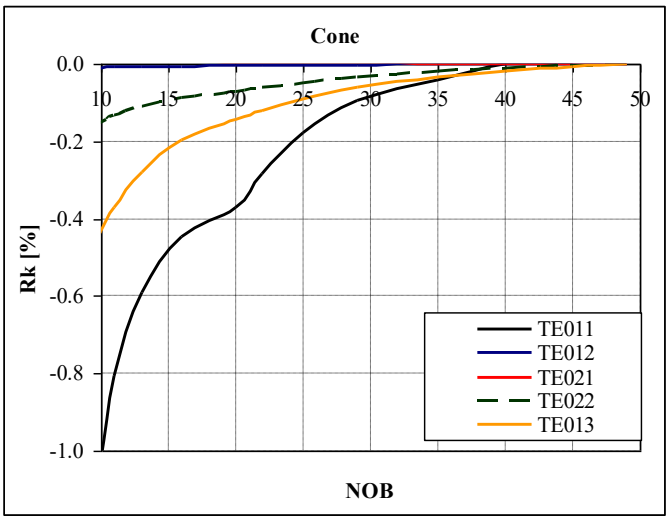

Fig. 10. Relative difference R_k as a function of number of regions in radial modes matching method (RMM)

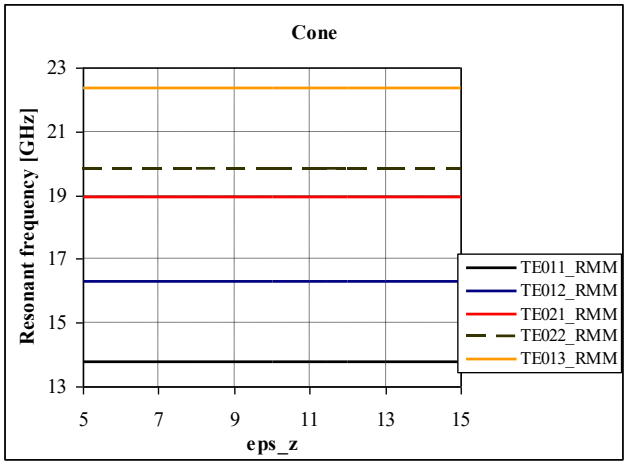

Fig. 11. Resonant frequency as a function of the permittivity ε_z for uniaxial anisotropic dielectric cone shaped resonator obtained by means of radial modes matching method (RMM)

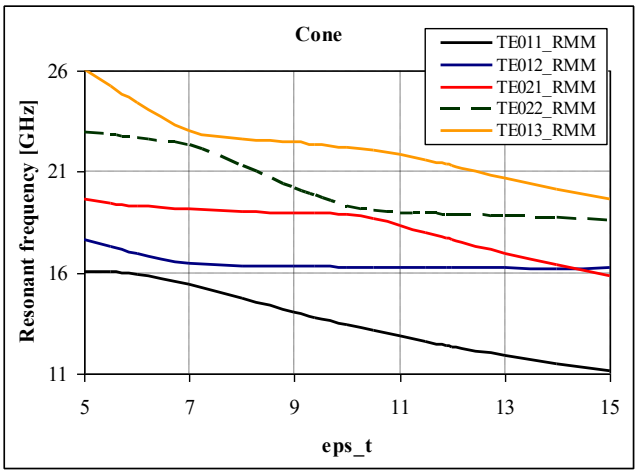

Fig. 12. Resonant frequency as a function of the permittivity ε_t for uniaxial anisotropic dielectric cone shaped resonator obtained by means of radial modes matching method (RMM)

Calculations were also made using the CST simulator. The results are presented in Figs 13 and 14 along with calculations using the radial modes matching method.

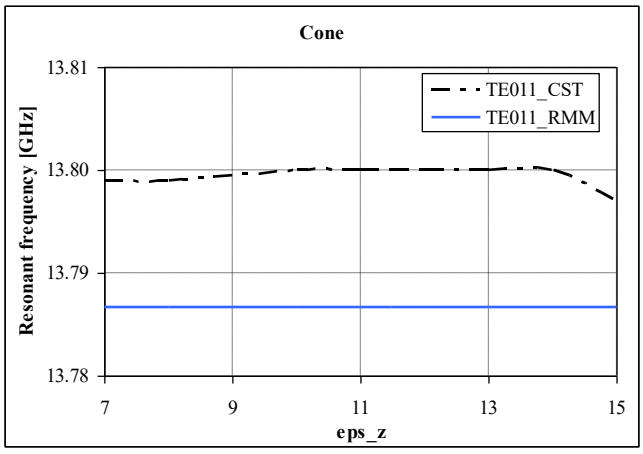

Fig. 13. Resonant frequency as a function of the permittivity ε_z for uniaxial anisotropic dielectric cone shaped resonator obtained by means of radial modes matching method (RMM) and CST simulator

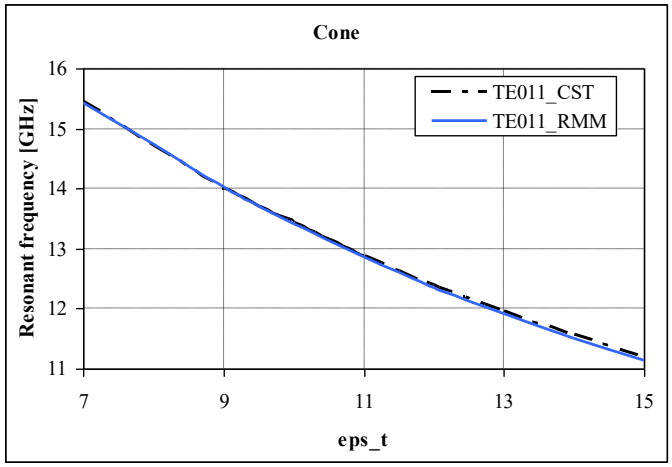

Fig. 14. Resonant frequency as a function of a permittivity ε_z for uniaxial anisotropic dielectric cone shaped resonator obtained by means of radial modes matching method (RMM) and CST simulator

Figs 15 and 16 show the relative difference R_f calculated by both programs for cone shaped resonator as a function of ε_z and ε_t.

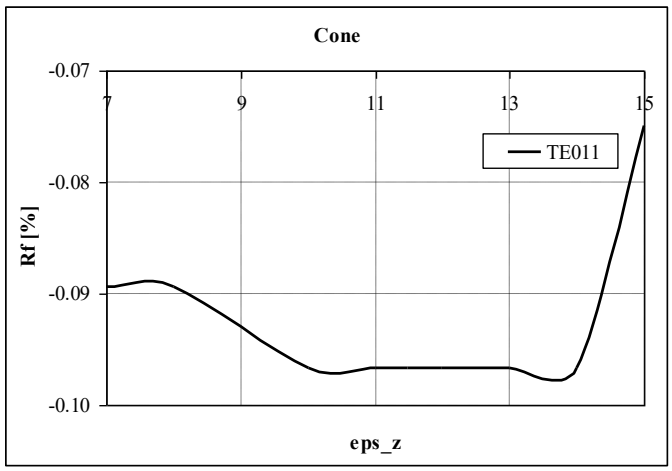

Fig. 15. The coefficient R_f as a function of a permittivity ε_z for uniaxial anisotropic dielectric conical resonator.

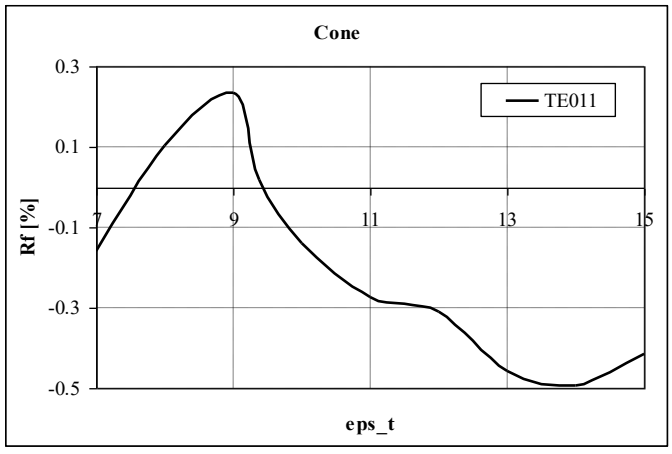

Fig. 16. The coefficient R_f as a function of a permittivity ε_z for uniaxial anisotropic dielectric conical resonator.

As seen, R_f varies from -0.1 to -0.07 percent with the change of ε_z and from -0.5 to 0.3 percent as a function of ε_t for TE_{011} mode. This is a very good agreement between the obtained results, especially considering the fact that the cone in the radial modes matching method was approximated using a cylinder and rings.

CONCLUSION

The paper presents the application of the radial modes matching method to determine the resonant frequencies of TE_{0mn} modes in a multilayered resonant structure containing uniaxial anisotropic materials. The solution of Maxwell's equations for TE_{0mn} modes is presented. A computer program was developed and launched enabling the analysis of structures composed of a maximum of 50 regions and 50 layers in each. This allows you to analyze complex structures such as a cone, a sphere, etc. The work deals with a cone shaped resonator as an example structure. The results of calculations as a function of the longitudinal and transverse components of tensor permittivity are presented, comparing them with the results obtained using the CST electromagnetic simulator. An analysis of the influence of the number of regions on the accuracy of calculations of resonant frequencies in the conical resonator was carried out. The obtained results allow the conclusion that the radial modes matching method can be successfully used to analyze axisymmetric structures with complex shapes.

REFERENCES

[1] J. Krupka, “Frequency domain complex permittivity measurements at microwave frequencies”; Measurement Science and Technology, vol.17. 2006, R55–R70. https://doi.org/ 10.1088/0957-0233/17/6/R01

[2] A. Abramowicz, J. Modelski, “Dielectric resonators and their applications”; PWN, 1990, (in Polish)

[3] W. Courtney, “Analysis and evaluation of a method of measuring the complex permittivity and permeability of microwave insulators”; IEEE Transactions on Microwave Theory and Techniques, vol. 18, no. 8, pp. 476-485, Aug. 1970. https://doi.org/10.1109/TMTT.1970.1127271

[4] S. B. Cohn, “Microwave bandpass filters containing high-Q dielectric resonators”, IEEE Transactions on Microwave Theory and Techniques, vol. 16, no. 4, pp. 218-227, Apr 1968. https://doi.org/10.1109/TMTT.1968.1126654

[5] J. K. Plourde and C .L. Ren, "Application of dielectric resonators in microwave components", IEEE Transactions on Microwave Theory and Techniques, vol. 29, no. 8, pp. 754–70, Aug. 1981. https://doi.org/10.1109/TMTT. 1981.1130444

[6] G. Lin, Y. K. Chembob, “Monolithic total internal reflection resonators for applications in photonics”, Optical Materials: X 2, vol. 2, 100017, May 2019. https://doi.org/10.1016/j.omx.2019.100017

[7] G. Lin, A. Coillet, Y. K. Chembo, “Nonlinear photonics with high-Q whispering gallery-mode resonators”, Advance in Optics and Photonics, vol. 9, no. 4, pp. 828–890, Dec 2017. https://doi.org/10.1364/AOP.9.000828

[8] Y. Kobayashi and M. Miura, “Optimum design of shielded dielectric rod and ring resonators for obtaining the best mode separation”, in Proc. IEEE MTT International Microwave Symposium, San Francisco, pp. 184–186, June 1984. https://doi.org/10.1109/MWSYM.1984.1131732

[9] J. Krupka, “Precise measurements of the complex permittivity of dielectric materials at microwave frequencies”, Materials Chemistry and Physics, vol. 79, no.2-3, pp. 195-198, April 2003. https://doi.org/10.1016/S0254-0584(02)00257-2

[10] A. Can Gungor, M. Olszewska-Placha, M. Celuch, J. Smajic, J. Leuthold, “Advanced modelling techniques for resonator based dielectric and semiconductor materials characterization”, MPDI Applied Sciences, vol. 10, 8533, Nov 2020. https://doi.org/10.3390/app10238533

[11] R. Saliminejad, M. R. Ghafourifard, “A novel and accurate method for designing dielectric resonator filter”, Progress in Electromagnetics Research B, Vol. 8, pp. 293–306, 2008. http://dx.doi.org/10.2528/PIERB08070602

[12] J. Krupka, A. Abramowicz, K. Derzakowski, “Design and realization of high–Q triple dielectric resonator filters with wide tuning range”, in Proc. 29th European Microwave Conference., pp. 103–106, Munich, Oct. 1999. https://doi.org/10.1109/EUMA.1999.338538

[13] A. Abramowicz, “Exact model of coupled dielectric resonators”, in Proc. 20th European Microwave Conference, pp. 1125–1130, Budapest, Sept 1990. https://doi.org/10.1109/EUMA.1990.336216

[14] S. K. K. Dash, T. Khan, A. De, “Modelling of dielectric resonator antennas using numerical methods: a review", Journal of Microwave Power and Electromagnetic Energy, vol. 50, no. 4, pp. 269-293, 2016. https://doi.org/10.1080/ 08327823.2016.1260677

[15] P. Abdulla, A. Chakraborty, “Rectangular waveguide-fed hemispherical dielectric resonator antenna”, Progress in Electromagnetics Research, vol.83: pp. 225-244, 2008. http://dx.doi.org/10.2528/PIER08050701

[16] H. Twu Chen, Y. T. Cheng, S. Y. Ke, „Probe-fed section-spherical dielectric resonator antennas”. in Proc. IEEE Asia Pacific Microwave Conference, vol. 2,.pp. 359-362, Nov. 1999. https://doi.org/10.1109/APMC.1999.829875

[17] S. Maj, J. Modelski, “Application of a dielectric resonator on microstrip line for measurement of complex permittivity”; in Proc. IEEE MTT International Microwave Symposium, San Francisco, 1984. https://doi.org/10.1109/MWSYM.1984.1131849

[18] J. Krupka, “Resonant modes in shielded cylindrical ferrite and single-crystal dielectric resonators”; IEEE Transactions on Microwave Theory and Techniques, Vol. 37, No. 4, pp. 691-696, April 1989. https://doi.org/10.1109/22.18841

[19] K. Derzakowski, A. Abramowicz, J. Krupka, “Whispering gallery resonator method for permittivity measurements”, Journal on Telecommunications and Information Technology, No.1, pp.43-47, 2002.

[20] S. Maj, ”Metoda wyznaczania częstotliwości drgań własnych i jej zastosowanie do analizy wielowarstwowego cylindrycznego rezonatora dielektrycznego”; PhD Thesis, Warsaw, 1987

[21] Y. Kobayashi, T. Sensu, “Resonant modes in shielded uniaxial-anisotropic dielectric rod resonators”; IEEE Transactions on Microwave Theory and Techniques, Vol. 41, No. 12, pp. 2198-2205, 1993. https://doi.org/10.1109/22.260706

[22] K. Derzakowski, “Full Wave Analysis of Multilayered Cylindrical Resonator Containing Uniaxial Anisotropic Media”, Progress in Electromagnetics Research M, vol. 101, pp. 101-115, 2021. https://doi.org/10.2528/PIERM20120804

[23] www.3ds.com - CST Studio - Electromagnetic field simulation software

[24] www.ansys.com - 3D Electromagnetic Field Simulator for RF and Wireless

[25] www.qwed.eu - Software for Electromagnetic Design